Mathematical modeling of heat and water transport in human respiratory tract

EVANGELIA DAVISKAS, IGOR GONDA, AND SANDRA D. ANDERSON
Department of Thoracic Medicine, Royal Prince Alfred Hospital, Camperdown 2050; and Department of Pharmacy, Sydney University, Sydney, New South Wales 2006, Australia

DAVISKAS, EVANGELIA, IGOR GONDA, AND SANDRA D. ANDERSON. *Mathematical modeling of heat and water transport in human respiratory tract.* J. Appl. Physiol. 69(1): 362–372, 1990.—Excessive heat and water losses from the airways are stimuli to asthma. To study heat and water vapor transport in the human respiratory tract, a time-dependent model, based on a single differential equation with an analytical solution, was developed that could predict the intra-airway temperatures and water vapor contents. The key feature is the dependence of the temperature and water vapor along the respiratory tract as a function of the air residence time at each location. The model assumes disturbed laminar flow leading to enhanced transport mechanisms and wall temperature profiles modeled according to experimental data (E. R. McFadden, Jr., B. M. Pichurko, H. F. Bowman, E. Ingenito, S. Burns, N. Dowling, and J. Solway. *J. Appl. Physiol.* 58: 564–570, 1985). It predicts that *1*) the air equilibrates with the wall before it reaches body conditions (37°C, 99.5% relative humidity); *2*) conditioning of the inspired air involves several generations, with the number depending on the respiratory conditions; and *3*) the walls of the upper airways are unsaturated, although it is difficult to judge at this state the depth of the respiratory tract affected.

exercise-induced asthma; respiratory heat exchange; respiratory water exchange; heat and water loss

THE CONDITIONING of the inspired air to 37°C and 99.5% relative humidity is essential for the normal function of the alveoli and for gas exchange. The geometry of the human respiratory tract ensures that these conditions are met by the time the air reaches the alveoli. The conditioning of the inspired air usually results in a net heat and water loss from the airways. Under normal circumstances nasal breathing is quite effective in conditioning the inspired air and also in minimizing the heat and water loss from the airways. When mouth breathing occurs instead of nasal breathing, as with exercise or hyperventilation, there is an abnormally high rate of heat and water loss from the airways. It is these excessively high rates of heat and water loss from the airways that are thought to be the stimuli by which exercise or hyperventilation induce an attack of asthma (1, 2, 4). Although it is clear that heat and water losses are putative stimuli to asthma, the anatomic site of this action is not known.

To study heat and water vapor transport in the human respiratory tract while conditioning the inspired air, it is necessary to obtain estimates of intra-airway temperatures and water contents. These are difficult to measure. Therefore mathematical models that can predict them are useful. The predicted intra-airway temperatures and water vapor concentrations can be used to calculate the local heat and water losses. Although the precise mechanism by which heat and water losses induce bronchoconstriction is not known, an increase in osmolarity is thought to be important (2). Therefore the local water loss could be further used to estimate the likely local changes in osmolarity for different inspired conditions and ventilations.

There have been a number of models recently published attempting to quantify heat and water vapor transport in the respiratory tract (22) for nasal breathing (8, 12) and for mouth breathing (9, 15, 28). In contrast to recent models (9, 15, 28), the present model is based on a single differential equation with an analytical solution. It is therefore much less demanding computationally. The key feature is the dependence of the temperature and water vapor along the respiratory tract as a function of the residence time of the air at each location. The residence time was shown experimentally to be the dominant factor in heat transport in the human respiratory tract (25). Because there is a limited range of experimental data available at present to validate these models, the results of the calculations should be viewed as a part of a refutable hypothesis.

Glossary

C_o	Water vapor concentration at entry of an airway, mg/l
C_p	Heat capacity of air, $kcal \cdot g^{-1} \cdot °C^{-1}$
C_w	Water vapor concentration at wall of an airway, mg/l
D_a	Additional diffusivity, cm^2/s
D_t	Thermal diffusivity, cm^2/s
D_w	Water vapor diffusivity in air, cm^2/s

f	Frequency of breathing, breaths/min
ΔH	Latent heat of vaporization, kcal/g
J_0	Bessel function of first kind of order 0
J_1	Bessel function of first kind of order 1
K	Thermal conductivity of air, kcal·cm^{-1}·s^{-1}·°C^{-1}
L	Cumulative length at middle of each airway, cm
P	Partial pressure of water vapor, Torr
r	Radial coordinate, $0 < r < R_w$
R_w	Radius of an airway, cm
t	Time, s
$\bar{t}$	Mean air residence time in an airway, s
T	Temperature, °C
T_E	Expired temperature, °C
T_I	Inspired temperature, °C
T_m	Temperature at lips, °C
T_o	Temperature at entry of an airway, °C
T_w	Temperature at wall of an airway, °C
v	Air velocity, cm/s
$\dot{V}$	Airflow rate, l/min
$\dot{V}E$	Ventilation, l/min
VT	Tidal volume, ml
W_E	Expired water vapor concentration at mouth, mg/l
W_I	Inspired water vapor concentration, mg/l
X_o	Temperature (T_o, °C) or water vapor concentration (C_o, mg/l) at entry of an airway
$X(r, \bar{t})$	Temperature (°C) or water vapor concentration (mg/l)
X_w	Temperature (T_w, °C) or water vapor concentration (C_w, mg/l) at wall of an airway
Y_0	Bessel function of second kind of order 0
z	Coordinate in direction of axis, cm
θ	Angular coordinate, rad
λ_n	nth positive zero roots of Bessel function, $J_0(\lambda_n R_w) = 0$
ρ	Density of air, g/cm^3

MODEL DEVELOPMENT

An energy and a mass balance equation of gas flowing through a circular tube gives a second-order partial differential equation, which describes the transport of heat and water vapor as a continuous function of time, radius, distance, and angle (16) as follows

$$\frac{\partial X}{\partial t} + v\frac{\partial X}{\partial z} = D\left(\frac{1}{r}\frac{\partial X}{\partial r} + \frac{\partial^2 X}{\partial r^2} + \frac{1}{r^2}\frac{\partial^2 X}{\partial \theta^2} + \frac{\partial^2 X}{\partial z^2}\right) \quad (1)$$

where D is either the thermal diffusivity of air (D_t) or the water vapor diffusivity in air (D_w); r is the radial coordinate; t is time; v is the velocity of gas, which in general is a function of radius; X is either temperature or water vapor concentration; z is the coordinate in the direction of the axis; and θ is the angular coordinate.

If it is assumed that diffusion is angle independent and that the transport of heat and water vapor is in the radial direction only, *Eq. 1* is simplified as

$$\frac{\partial X}{\partial t} = D\left(\frac{1}{r}\frac{\partial X}{\partial r} + \frac{\partial^2 X}{\partial r^2}\right) \quad (2)$$

Equation 2 thus describes the heat and water vapor transport as a continuous function of radius and time. Its analytical solution gives the temperature or water vapor concentration as a function of tube radius and time for different inspired conditions (see APPENDIX A)

$$X(r,\bar{t}) = X_w - 2(X_w - X_o)\sum_{n=1}^{\infty}\frac{J_0(\lambda_n r)e^{-D\lambda_n^2\bar{t}}}{\lambda_n R_w J_1(\lambda_n R_w)} \quad (3)$$

where J_0 and J_1 are the Bessel functions of the first kind of order 0 and 1, respectively; r is the radial distance, which can vary from 0 to R_w; R_w is the radius of the airway; $\bar{t}$ is the air residence time in an airway; X_o is the entry temperature (T_o) or water vapor concentration (C_o); $X(r,\bar{t})$ is the temperature or the water vapor concentration; X_w is the wall temperature (T_w) or the wall water vapor concentration (C_w); and λ_n is the nth positive zero roots of the Bessel function $J_0(\lambda_n R_w) = 0$.

The mean temperature or water vapor concentration over the cross-sectional area can be represented by the following equation (16)

$$\text{mean } X(r,\bar{t}) = \frac{1}{\pi R_w^2}\int_0^{R_w} X(r,\bar{t})\, 2\pi r\, dr \quad (4)$$

Substituting $X(r,\bar{t})$ from *Eq. 3* and integrating *Eq. 4* gives (see APPENDIX A)

$$\text{mean } X(r,\bar{t}) = X_w - \frac{4(X_w - X_o)}{R_w^2}\sum_{n=1}^{\infty}\frac{e^{-D\lambda_n^2\bar{t}}}{\lambda_n^2} \quad (5)$$

The wall conditions are important parameters in *Eqs. 3* and *5*. The local gradients between the mucosa and the inspired air traveling through the respiratory tract are dependent on the mucosal and the inspired conditions. In contrast to the inspired conditions, i.e., T_I and inspired water (W_I) or relative humidity, the mucosal conditions are not directly known. For simplicity, it is assumed here that the temperature and the water vapor concentration along the wall of each individual airway remain constant. In reality, the wall conditions are not constant; they change with time and location. However, because the main heat and water source is the blood and the local blood flow is not known, the rate of the heat and water supply cannot be known with accuracy. Therefore the wall temperatures were modeled, using an iterative procedure, to obtain agreement with experimental data (20). This procedure is clearly a compromise; it enables us to model the wall conditions while avoiding the coupled dynamic problem of water and heat transport at the wall. On the other hand, it restricts the predictions of the model to the vicinity of the respiratory regimens of the experiments used to obtain the wall conditions. The temperature along the wall of each airway was assumed to be constant and equal to the calculated wall temperature at the middle of the longitudinal distance of each airway. This was considered to be a good approximation to the real airway temperature. The variation in the T_w along the airways was found to be a function of T_I and breathing pattern (see APPENDIX B) at end inspiration

$$T_w = T_m + (37 - T_m)[1 - e^{-(0.00564\dot{V}E + 0.276)L/\dot{V}}] \quad (6)$$

at end expiration

$$T_w = T_m + (37 - T_m)[1 - e^{-(0.00564\cdot\dot{V}E + 0.336)L/\dot{V}}] \quad (7)$$

where L is the cumulative length at the middle of each airway (cm), T_m is the temperature at the lips (°C; APPENDIX B), $\dot{V}$ is the airflow rate in the corresponding airway (l/min), and $\dot{V}E$ is the ventilation (l/min).

Thus if T_w of each airway is kept constant, T_w along the respiratory tract, for the modeling purpose, increases in a stepwise manner. The water vapor concentration (C_w) at the wall was modeled assuming various degrees of saturation at T_w (T_w was fitted as described above). Initially, 99.5% saturation was assumed, as one would expect for the vapor pressure in equilibrium with blood serum (7).

The thermal diffusivity of air is defined as

$$D_t = \frac{K}{\rho C_p} \text{ (cm}^2\text{/s)}$$

where C_p is the heat capacity of air, K is the thermal conductivity of air, and ρ is the density of air.

In reality, K and C_p of air are dependent on the temperature and the humidity of the air. D_w is also temperature dependent. However, the values of D_t and D_w used were assumed to be constant here, 0.232 and 0.267 cm^2/s, respectively (8). These constants are for dry air at 37°C. Other workers found that the temperatures and water vapor concentrations predicted with constant parameters at 37°C differed by <3% from those predicted with temperature-dependent parameters (8). Therefore, corrections for humidity and temperature were ignored, as they would unnecessarily complicate the model and would not contribute significantly to accuracy.

The airflow was modeled as laminar in the mouth in accordance with Swift and Proctor (26). The airflow was assumed to be disturbed laminar in all airways, except the mouth, during inspiration. It is known that disturbed laminar airflow exists everywhere in the lung because of the severe disturbances through the airways caused by bends, changes in airway cross section, and bifurcations (21). Every time the air travels around a bend, secondary flows are created. Two secondary flows are formed during inspiration, where airflow from the parent airway divides into the two daughter airways, and four secondary flows are found during expiration, where the airflows from the daughter airways join into the parent airway (23). The secondary flows increase the mixing of the air, since elements from near the wall are swept toward the center (21). This justifies the use of an additional diffusivity (D_a) applied in the whole cross section of the airway rather than in the core only (8). Thus the effective diffusivity constant was calculated as the sum $D + D_a$. During inspiration, apart from the disturbed laminar flow due to secondary flows, there is turbulence generated by the glottis. This is present even at resting ventilation and increases as ventilation increases (21). Also the turbulence is convected downstream until viscous forces are able to dissipate the associated eddies (29). It was estimated that during normal breathing complete dissipation does not occur until the 7th generation (17). At high ventilations, where the air velocity increases two to six times, the flow becomes turbulent in the airways. Therefore this turbulence and the turbulence induced by the glottis dissipates even deeper in the lung at high ventilations (29). Consequently, air mixing should be enhanced in the airways past the larynx. This was modeled by having a higher additional diffusivity constant, for the same flow rate, than the constant used in the pharynx and larynx (see *Eq. 9*). During expiration, at all locations all the air coming from the tracheobronchial tree and the alveoli was assumed to exchange heat and water with the additional diffusivities, according to *Eq. 9* below. The air coming from the pharynx and larynx had the additional diffusivity according to *Eq. 8* below. This equation was also used for heat and water transport during inspiration in these two locations. The additional diffusivity was modeled to obtain agreement with experimental data (20) and was found to be dependent on airflow rate (see APPENDIX C)

$$D_a = 0.177\ \dot{V}^{0.41} \text{ for pharynx and larynx (cm}^2\text{/s)} \quad (8)$$

$$D_a = 0.354\ \dot{V}^{0.41} \text{ for glottis and rest of airways (cm}^2\text{/s)} \quad (9)$$

where $\dot{V}$ is the airflow rate (ml/s).

If the airflow is assumed to be a square wave, then the mean air residence time ($\bar{t}$) in an airway was calculated as follows

$$\bar{t} = \frac{\text{airway volume}}{\text{mean airflow rate in airway}} \text{ (s)}$$

The geometry of the conducting airways was approximated by straight circular tubes according to the model of Weibel (31). The radii of the pharynx and larynx were based on results of computer-aided tomography scan measurements (S. Chan, personal communication). The radius of the mouth, assumed to be approximated by a circular tube, was estimated from an average volume (20 ml) and an average axial length (8 cm) to be 0.89 cm. This is in good agreement with the dimensions recommended by Ultman (30). The glottis was treated as a tube of radius 5.59 mm, which was derived from the mean of the peak cross-sectional areas that it reaches during the respiratory cycle (3).

The model was programmed in Fortran and run on a digital computer (PDP 11-73, Digital Equipment, Maynard, MA).

VALIDATION STUDIES FOR EXPIRED TEMPERATURE AND WATER

The common laboratory measurements are the temperature and water vapor concentration of the airstream as it is expired at the mouth. Therefore, comparison of the predicted expired airstream temperatures and water vapor concentrations with the experimental data at the mouth is important. Experimental temperature and water vapor concentration of the expired air at the mouth were obtained as follows.

Five healthy subjects exercised at a submaximal work load on a bicycle ergometer (Elema-Schonander, Solna,

Sweden) for 10–15 min. The inspired air temperature increased during exercise from 26 to 42°C and contained between 6.5 and 9 mg H_2O/l. The subjects breathed through a two-way valve of low resistance (Hans-Rudolph no. 2700, Kansas City, MO). The valve was divided in half by cutting and inserting a thin layer of perspex through the body and mouthpiece of the valve, separating the inspiratory from the expiratory air. T_I was measured by placing a thermistor (Yellow Springs no. 401, Yellow Springs, OH) 4 cm before the inspiratory valve. The expired temperature (T_E) was measured using a rapid thermistor (Yellow Springs model 520). The rapid thermistor had a 90% response time of 1.6 and 0.92 s for inspired temperatures between 20–30°C and 30–40°C, respectively, when the flow rate was 100 l/min. The response time of the thermistor was sufficiently rapid for the correct temperature to be recorded for most frequencies of breathing during exercise, which were usually <30 breaths/min. The thermistor was placed in the expiratory side of the divided valve and was not influenced by the inspired air. The measurements commenced once the subject was exercising steadily, as observed by the pattern of the output variables. T_I was increased by ~1°C/min. The increases in T_I did not cause much change in T_E. The inspired and expired water vapor pressure was measured using a mass spectrometer with a heated probe (Centronics model 200, MGA, Kent, UK). The mass spectrometer had a 90% response time of <100 ms. The probe was placed in the expiratory part of the divided valve, and care was taken to ensure that it did not interfere with the thermistor. The expired air passed through a mixing chamber into a 350-liter Tissot gasometer (W. E. Collins, Braintree, MA). The analog signals were displayed on an eight-channel recorder (Devices M-19, Herts, UK) and then passed through an analog-to-digital converter (Digital Equipment) into a computer (PDP 11-03, Digital Equipment). The computer was programmed in Fortran for on-line real time analysis of the data for each minute (Scientia, Sydney, Australia). Values for inspired and expired temperature, expired water, frequency of breathing, tidal volume, and ventilation were displayed each minute. The ventilation remained steady throughout exercise for each subject. The values for water vapor pressure were converted to milligrams of water per liter as follows

$$\text{water vapor concentration} = \frac{(P/760)18{,}000}{0.082053(273 + T)} \text{ (mg/l)}$$

where P is the partial pressure of water vapor (Torr) and T is the temperature (°C).

RESULTS

The intra-airway temperatures were calculated for T_I = 26.7°C, W_I = 8.8 mg/l, and $\dot{V}E$ = 15, 30, 60, and 100 l/min, which are the experimental conditions used in the development of the model. The calculated temperatures reproduced the experimental data (20) within experimental errors at five locations at the end of inspiration and expiration and for ventilations of 15, 30, 60, and 100 l/min (Table 1). The calculated mean intra-airway temperatures throughout the respiratory tract at the end of

TABLE 1. *Experimental and calculated values of intra-airway temperatures at end inspiration and expiration at four ventilations for different locations in human respiratory tract*

Ventilation, l/min	Location	Mean Airstream Temperatures, °C			
		Inspiration		Expiration	
		Experimental	Model	Experimental	Model
15	End glottis	32.0±0.5	32.1	32.9±0.4	33.4
	End trachea	33.2±0.5	33.1	34.2	33.9
	End 2nd gen.	33.8	33.9	35.0	34.6
	End 4th gen.	34.3±0.5	34.6	35.4	35.6
	End 6th gen.	35.5±0.3	36.0	36.3±0.6	36.7
30	End glottis	31.2	31.1	32.6	32.7
	End trachea	32.1	32.3	33.4	33.2
	End 2nd gen.	33.0	33.0	34.0	33.6
	End 4th gen.	33.9	33.6	35.0	34.5
	End 6th gen.	35.5	35.0	36.2	36.1
60	End glottis	30.3	30.2	31.7	32.0
	End trachea	31.4	31.3	32.9	32.3
	End 2nd gen.	32.1	32.1	33.0	32.7
	End 4th gen.	32.9	32.7	34.0	33.5
	End 6th gen.	34.6	34.1	35.3	35.2
100	End glottis	29.2±0.5	29.2	30.4±0.3	31.2
	End trachea	30.2±0.4	30.3	31.5	31.5
	End 2nd gen.	31.0	31.1	32.0	31.9
	End 4th gen.	31.6±0.5	31.7	33.2	32.7
	End 6th gen.	33.9±0.8	33.2	34.9±0.8	34.5

Experimental values are means ± SE from McFadden et al. (20). Gen., generation.

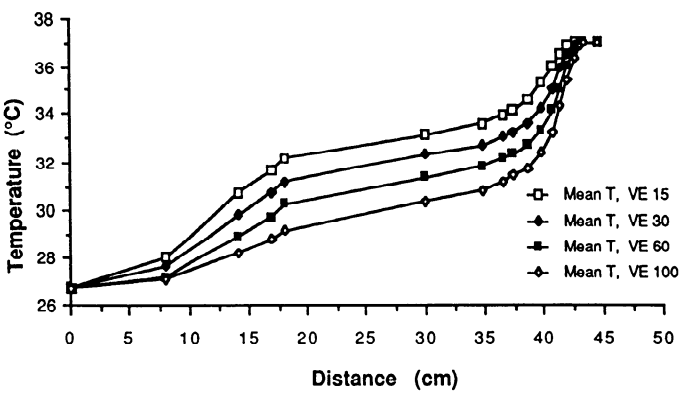

FIG. 1. Theoretical intra-airway mean temperature (T) profiles at end of inspiration for ventilations (VE) of 15, 30, 60, and 100 l/min. Inspired temperature, 26.7°C; inspired water content, 8.8 mg/l.

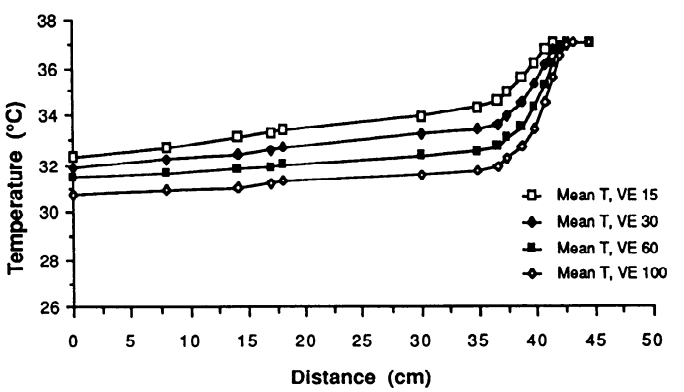

FIG. 2. Theoretical intra-airway mean temperature profiles at end of expiration for ventilations of 15, 30, 60, and 100 l/min. Inspired temperature, 26.7°C; inspired water, 8.8 mg/l.

inspiration and expiration are illustrated in Figs. 1 and 2, respectively. Comparisons of the mean, axial, experimental, and wall temperatures are shown in Figs. 3–6 for ventilation of 15 and 100 l/min at the end of inspiration and expiration. The predicted expired temperatures at the mouth for T_I varying from 26 to 34.9°C and W_I varying from 6.78 to 8.2 mg/l were compared with the experimental data from the five subjects in this study (Table 2). This is illustrated in Fig. 7.

The water vapor concentrations along the respiratory tract were predicted for T_I varying from 26 to 34.9°C and W_I varying from 6.78 to 8.2 mg/l so that comparison could be made with the experimental data at mouth. Results were predicted assuming initially that the relative humidity along the wall of the airways was 99.5% (Table 2) and with the wall of the mouth, pharynx, and larynx at relative humidity <99.5% (Table 3). Figures 8 and 9 illustrate the intra-airway mean, axial, and wall water vapor concentrations for T_I = 28.4°C, W_I = 7.85 mg/l, and $\dot{V}E$ = 15.2 l/min when the wall water vapor concentrations at mouth, pharynx, and larynx were set to 91, 93, and 96% of the saturation at the wall temperature, respectively. Figure 10 illustrates the percent relative humidity of the expired air at the mouth for these conditions. Also, Figs. 11 and 12 illustrate the intra-airway percent relative humidity at the end of inspiration and expiration, respectively.

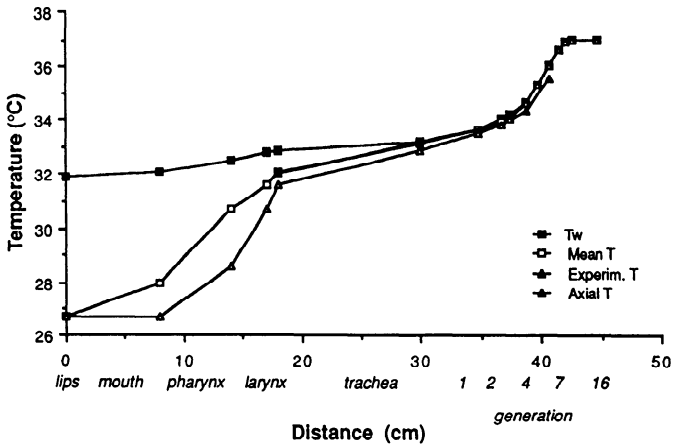

FIG. 3. Comparison of theoretical intra-airway mean and axial temperatures with wall (T_w) and experimental airstream temperatures at end of inspiration. Inspired temperature, 26.7°C; inspired water, 8.8 mg/l; ventilation, 15 l/min.

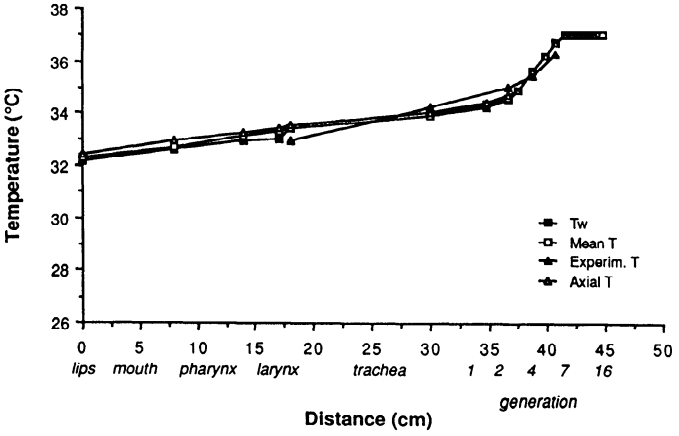

FIG. 4. Comparison of theoretical intra-airway mean and axial temperatures with wall and experimental airstream temperatures at end of expiration. Inspired temperature, 26.7°C; inspired water, 8.8 mg/l; ventilation, 15 l/min.

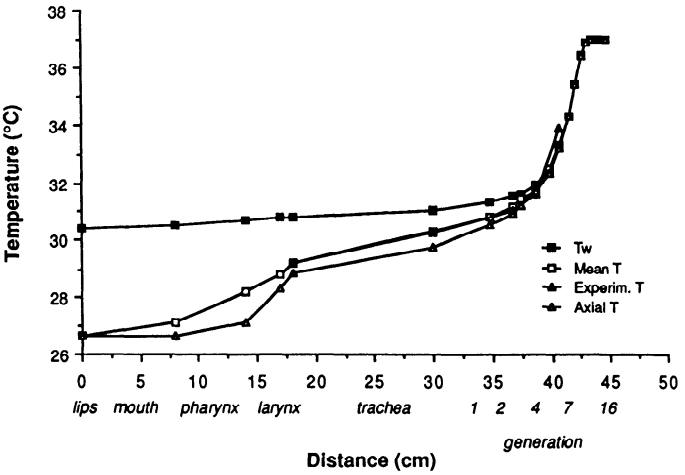

FIG. 5. Comparison of theoretical intra-airway mean and axial temperatures with wall and experimental airstream temperatures at end of inspiration. Inspired temperature, 26.7°C; inspired water, 8.8 mg/l; ventilation, 100 l/min.

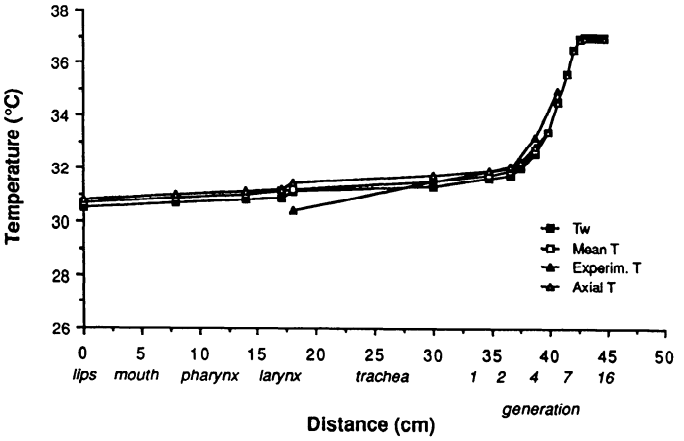

FIG. 6. Comparison of theoretical intra-airway mean and axial temperatures with wall and experimental airstream temperatures at end of expiration. Inspired temperature, 26.7°C; inspired water, 8.8 mg/l; ventilation, 100 l/min.

DISCUSSION

The iterative procedure to find the wall conditions led to a satisfactory agreement between the calculated and experimental intra-airway temperatures (20; Table 1). This helped toward modeling the airway wall temperatures, which can be now predicted with some confidence as a function of inspired temperature, cumulative airway length, and airway flow rate when the inspired water vapor is close to 8.8 mg/l and the inspired temperature is in the range of 26–35°C. The assumption about higher wall temperatures during expiration can be justified by the fact that they represent temperatures toward the end of expiration. In addition, if steady state at the wall is established within 20% of the inspiratory and expiratory time (12, 13), it is reasonable to expect higher wall temperatures at the wall during the 80% of the expiratory

TABLE 2. *Comparison of predicted temperatures and water vapor contents at mouth with experimental values*

T_I, °C	W_I, mg/l	$\dot{V}_E$, l/min	f	V_T, ml	Experimental Values		Predicted Values	
					T_E, °C	W_E, mg/l	T_E, °C	W_E, mg/l
26.0	7.72	15.3	15	1,020	31.9	*	32.1	33.6
26.0	6.78	13.5	16	844	31.8	*	32.2	33.7
27.0	8.20	18.0	12	1,503	32.7	34.1	32.3	33.9
27.0	7.72	19.0	19	1,000	32.5	31.0	32.2	33.8
28.0	7.72	18.1	15	1,209	32.3	33.7	32.5	34.3
28.3	6.78	30.2	28	1,078	32.8	31.0	32.3	33.9
28.4	7.85	15.2	16	947	32.6	31.6	32.7	34.6
28.5	7.72	19.2	19	1,010	32.6	30.6	32.6	34.5
29.5	7.72	18.6	20	931	32.8	32.7	32.8	34.9
29.5	6.78	21.4	26	821	32.5	30.5	32.8	34.8
30.6	7.72	19.8	21	941	33.0	32.3	33.1	35.4
30.6	8.20	15.6	9	1,731	33.1	31.1	33.2	35.5
30.8	7.72	19.3	15	1,287	32.3	33.7	33.1	35.5
30.8	7.85	21.2	16	1,322	32.7	36.6	33.1	35.4
30.8	7.85	22.4	15	1,493	33.2	35.0	33.0	35.3
30.9	6.78	21.7	27	805	32.7	32.6	33.1	35.4
31.3	6.78	19.3	21	921	32.9	31.6	33.2	35.7
31.4	7.72	18.7	20	936	33.3	31.3	33.3	35.8
32.0	6.78	19.0	25	760	32.9	32.4	33.4	36.0
32.0	7.85	17.7	18	983	33.3	32.4	33.4	36.1
32.5	7.72	17.6	15	1,175	32.5	33.7	33.6	36.3
33.0	7.85	16.8	15	1,118	32.9	35.3	33.7	36.5
33.5	8.20	18.4	14	1,314	33.2	31.6	33.6	36.7
33.5	7.72	26.3	23	1,141	33.2	32.0	33.6	36.4
33.6	7.72	19.8	15	1,321	33.0	33.5	33.8	36.7
34.0	8.20	28.1	12	2,382	33.5	33.9	33.7	36.5
34.1	6.78	22.5	28	801	32.9	33.6	33.8	36.8
34.1	7.85	17.8	19	935	33.0	34.5	33.7	37.0
34.2	6.78	21.0	26	807	33.1	32.1	33.9	36.9
34.9	7.72	26.3	22	1,197	33.4	30.3	33.9	37.0

Predicted values are from present model, with relative humidity = 99.5% at the wall throughout the whole respiratory tract. * Values not available.

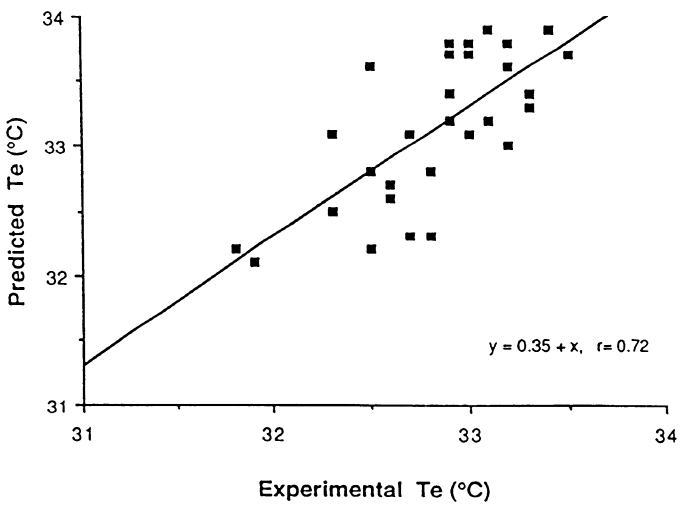

FIG. 7. Comparison of theoretical mean T_E at mouth with experimental temperatures. Range of inspired temperature, 26–34.9°C; inspired water, 6.78–8.2 mg/l; number of subjects, 5.

time when air at 37°C passes over the mucosa that was cooled during inspiration. Therefore the modeled wall temperatures during the end inspiration and expiration can realistically represent the wall temperatures for the whole inspiratory and expiratory time. In the models of Hanna and Scherer (12, 13) and Ferron et al. (8, 9) no

TABLE 3. *Experimental and predicted water vapor concentration varying the wall saturation at mouth, pharynx, and larynx*

Experimental							Predicted				
T_I, °C	W_I, mg/l	$\dot{V}_E$, l/min	f	V_T, ml	T_E, °C	W_E, mg/l	T_E, °C	W_E, mg/l	% RH		
									M	P	L
27.0	7.72	19.0	19	1,000	32.5	31.0	32.2	31.2	91	93	96
28.4	7.85	15.2	16	947	32.6	31.6	32.7	31.8	91	93	96
28.3	6.78	30.2	28	1,078	32.8	31.0	32.3	31.1	90	93	96

M, mouth; P, pharynx; L, larynx; RH, relative humidity.

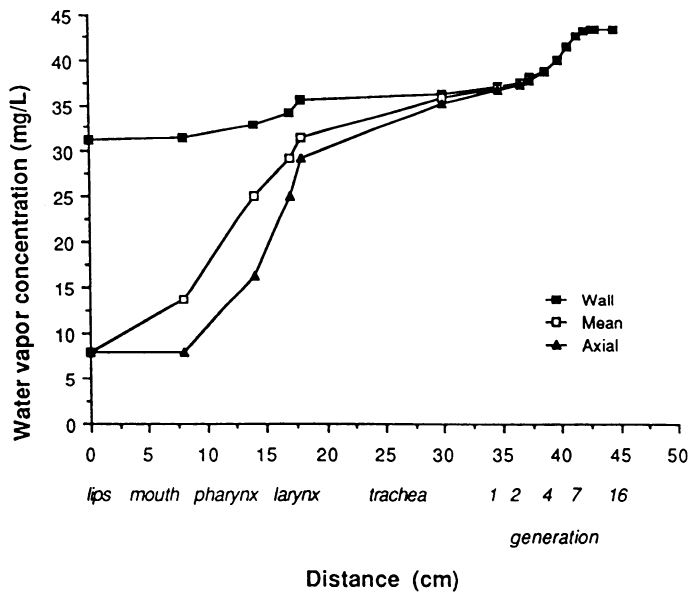

FIG. 8. Theoretical intra-airway mean, axial, and wall water vapor concentration profiles at end of inspiration. Inspired temperature, 28.4°C; inspired water, 7.85 mg/l; ventilation, 15.2 l/min. Relative humidity at wall of mouth, pharynx, and larynx was 91, 93, and 96%, respectively.

change in the local temperatures at the wall during the whole respiratory cycle was assumed. This seems unrealistic for the reasons explained above.

The calculated airstream temperatures converge toward the wall during inspiration as the air travels deeper inside the respiratory tract, which is in agreement with Ferron et al. (8, 9) and Ingenito et al. (14). This is not in agreement with Hanna and Scherer (13), who showed a divergence between the airstream and wall temperature profiles. During expiration, the calculated airstream and wall temperatures are almost in equilibrium, as suggested by McFadden et al. (19).

As seen in Figs. 1 and 2, the local airstream temperature decreases as ventilation increases from 15 to 100 l/min when the T_I and W_I are 26.7°C and 8.8 mg/l, respectively. Local temperature differences close to 2.8°C, between ventilations of 15 and 100 l/min, were found in *generations 0–6.* These local temperature differences are consistent with the experimental data (20). Local temperature differences close to 1.5°C were predicted by Ingenito et al. (15), using a model based on the energy and mass balance at the air-mucus interface, for T_I = 26.7°C and W_I = 11.84 mg/l when ventilation increased from 15 to 60 l/min. In contrast, Ferron et al.

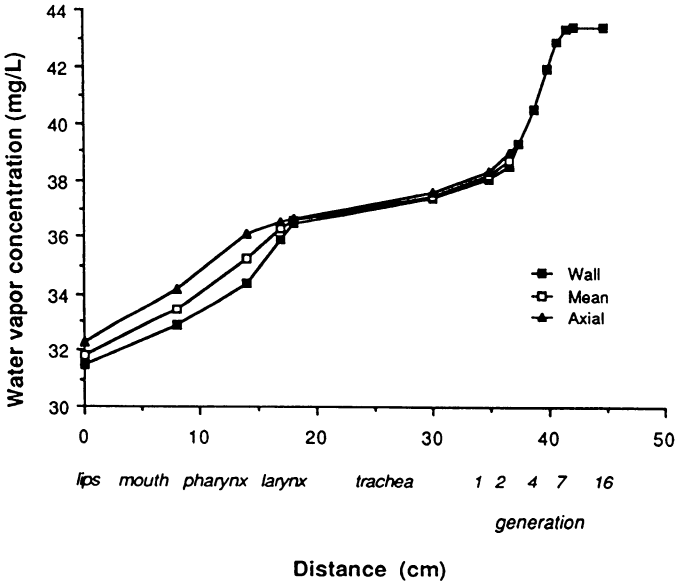

FIG. 9. Theoretical intra-airway mean, axial, and wall water vapor concentration profiles at end of expiration. Inspired temperature, 28.4°C; inspired water, 7.85 mg/l; ventilation, 15.2 l/min. Relative humidity at wall of mouth, pharynx, and larynx was 91, 93, and 96%, respectively.

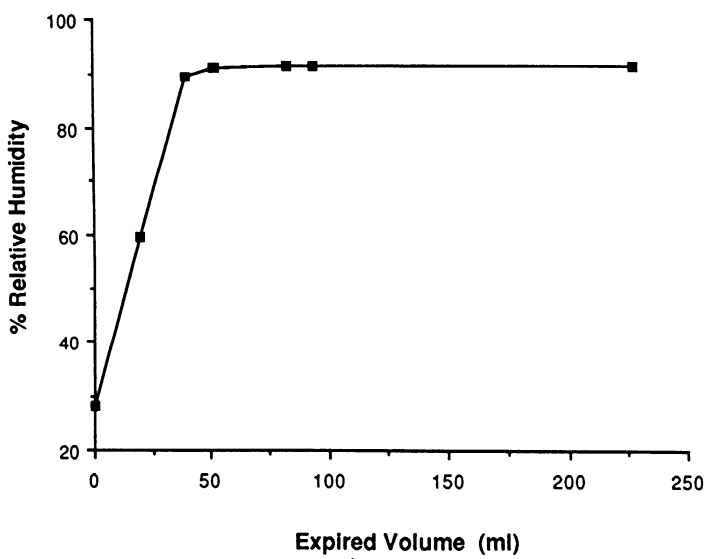

FIG. 10. Relative humidity of expired air at mouth. Inspired temperature, 28.4°C; inspired water, 7.85 mg/l; ventilation, 15.2 l/min.

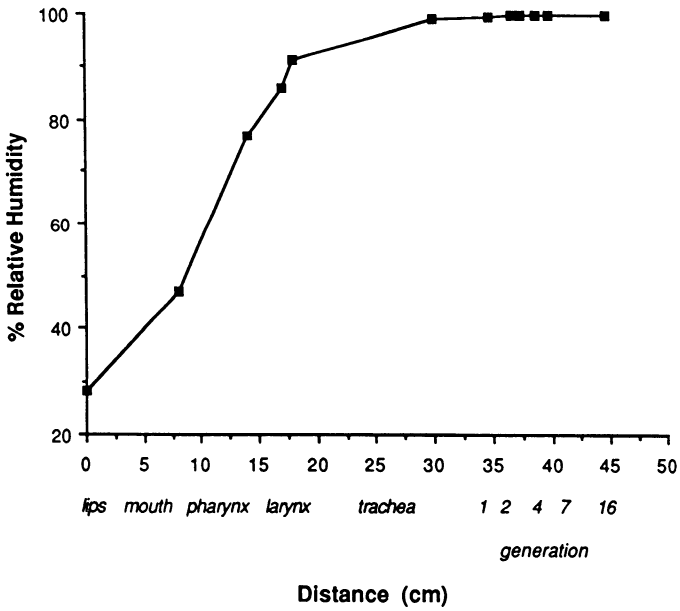

FIG. 11. Theoretical intra-airway mean relative humidity at end of inspiration. Inspired temperature, 28.4°C; inspired water, 7.85 mg/l; ventilation, 15.2 l/min.

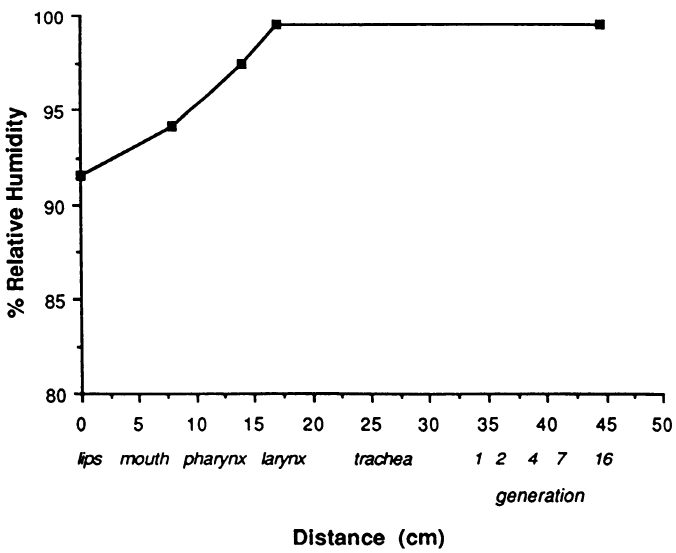

FIG. 12. Theoretical intra-airway mean relative humidity at end of expiration. Inspired temperature, 28.4°C; inspired water, 7.85 mg/l; ventilation, 15.2 l/min.

(9), using a steady-state model, predicted that the mean air temperature at any location differed by <0.5°C when ventilation changed from 7.5 to 22.5 l/min.

At all ventilations there was a steep increase in the air temperature in the extrathoracic airways up to the level of the pharynx and also in *generations 4–7*. This could be explained by the fact that the temperature gradient between the air and the wall is greatest in the extrathoracic airways and that the radius of the airways decreases significantly past the 4th generation while the air residence time increases. The temperature profiles are very similar to the experimental profiles (20) and to the predicted profiles of Ingenito et al. (15). Hanna and Scherer (12), using a model based on a steady-state energy and mass balance at the air-mucus interface, predicted qualitatively similar intra-airway temperature profiles to ours for nasal breathing. They predicted the first rapid increase in the temperature to occur within the nasal cavity and the second rapid increase to occur in the trachea and the central airways.

The present model predicts that of the total warming of the inspired air (T_I = 26.7°C, W_I = 8.8 mg/l, 35% relative humidity), 52, 43, 34, and 24% were completed at the level of the glottis for ventilations of 15, 30, 60, and 100 l/min, respectively. The model by Ingenito et al. (15) predicted similar results.

A unique finding of the present model was that at all ventilations, for the above conditions, the air reached equilibrium with the wall before it reached 37°C, the location of which depended on ventilation. When venti-

lation increased from 15 to 100 l/min, the inspired air equilibrated with the wall at the 4th (34.6°C) and 7th (34.3°C) generations and reached 37°C at the 9th and 11th generations, respectively. Therefore, as ventilation increases, if the inspired conditions are kept constant, at inspiration the air would have to travel deeper in the lung to reach equilibrium with the wall temperature as well as to reach 37°C. This is in agreement with Solway et al. (25), who found that as the velocity of air increases, although the heat transfer coefficient increases, the decrease in the local residence time is the dominant factor, which results in less local heat transfer. When ventilation increases from 15 to 100 l/min, the air has to travel 0.85 cm further before it reaches 37°C according to this model. However, the extra number of airways that became involved over this short distance is 1,536. This difference in airway recruitment resulted from the balance of the airway airflow rate, residence time, and additional diffusivity. At expiration, as ventilation increases, the local residence time is reduced and the recovery of heat is smaller. Therefore, because of the high frequency of breathing and the reduced recovery of heat during expiration, the wall temperatures become cooler as ventilation increases. This could account for the lower local temperatures, the increase in the number of airways involved in the conditioning of the air, and the shift of the equilibrium with the wall temperature deeper in the lung.

There was a linear correlation ($r = 0.72$) between the calculated and the experimental temperatures at the mouth (Table 2; Fig. 7) for the following conditions: T_I = 26–34.9°C, W_I = 6.78–8.2 mg/l, and $\dot{V}E$ = 13.5–28.1 l/min. The calculated temperatures would generally overpredict the experimental data by a constant factor of 0.35°C. This could be explained at least partly by the incomplete response of the thermistor, especially at higher flow rates. However, the correlation between the experiment and theory had a slope equal to 1 for the above inspired conditions. The maximum discrepancy found was 1.1°C. The wall conditions were derived from a restricted range of experimental inspired temperatures and water content values. The model systematically overpredicts when $T_I > T_E$. It is likely that the formula for the wall temperatures is incorrect when such an inversion of temperatures occurs. Computations for inspired water content outside the range in this paper (6.7–9 mg/l) show greater discrepancy with experimental data. This is likely to be the result of enthalpy of vaporization (or condensation) affecting the wall temperatures.

It was deduced from the predicted results that the expired temperatures at the mouth decrease as ventilation increases for the same inspired conditions (see APPENDIX B). This contradicted the empirical equation $T_E = 26.0 + 0.25\ T_I$ (11), which was assumed to be independent of ventilation and applied to a temperature range of 10–40°C and ~50% saturation. T_E calculated from Varene's equation for a T_I of 26.7°C was 32.7°C. T_E predicted by the present model, for ventilations of 15 and 100 l/min, was 32.3 and 30.7°C, respectively, and was consistent with experimental observations (Table 2). The temperature at the lips was considered to be the same as the expired temperature. This was the reason why Varene's equation was modified when used for the prediction of the temperature of the lips (APPENDIX B).

It was also found that when the water vapor concentration along the wall was 99.5% saturated at all airways, the predicted expired water vapor concentrations (W_E) at the mouth were significantly higher than the experimental data. The calculated W_E was found to vary from 33.9 to 37 mg/l when T_I and W_I were changed between 26 to 34.9°C and 6.78 to 8.2 mg/l, respectively. Because during expiration the airstream temperature or water vapor concentration was calculated to be almost at equilibrium with the wall condition, the expired water vapor concentration at the mouth was always 99.5% saturated at the expired temperature. This was not the experimental finding (Table 2). Most of the experimental water vapor concentrations were close to 90% saturation. There are also other experimental data (1, 2, 18, 28) that show that the expired temperature is not fully saturated with water vapor. Therefore the saturation along the wall could not always be 99.5%. The questions that arose from this were *1*) how many airways have their wall relative humidity <99.5%, *2*) what is their saturation, and *3*) what are the factors that control this?

Initially, the saturation was varied only in the mouth. It was found that when its saturation was <90% there was good agreement with the experimental data for W_E. It was not reasonable, though, to assume that only the mouth had an unsaturated wall. The well-known sensation of dryness at the pharynx when breathing through the mouth would support this. When the wall water vapor concentration was changed at mouth, pharynx, and larynx, the burden was spread, and there was good agreement between the calculated expired water vapor concentration and the experimental data (Table 3). Changing the wall saturation at mouth, pharynx, and larynx affected the results at these locations mainly and slightly at the next couple of generations. It did not affect the location where the airstream equilibrated with the wall or reached 43.42 mg/l (99.5% saturation at 37°C). This finding indicates that the transfer of heat and water is really rapid.

The intra-airway water vapor concentrations (Fig. 8), calculated for air inspired with T_I = 28.4°C, W_I = 7.85 mg/l (28% relative humidity), and $\dot{V}E$ = 15.2 l/min (Table 2), showed that the airstream temperature and water vapor concentration equilibrated with the wall at the same location (4th generation, 34.8°C, 38.7 mg/l) and reached 43.42 mg/l at the 9th generation at the location where the airstream reached 37°C. At expiration, both the temperature and the water vapor concentration (Fig. 9) were at equilibrium with the wall up to the 3rd generation (35.1°C, 39.3 mg/l). The relative humidity of the expired air at the mouth (Fig. 10), for the same conditions, increased from 28 to 91.55% during the expiration of the last inspirate volume (~80 ml). A plateau was reached within 0.164 s, which is 8.7% of the total expiratory time. This value was almost at equilibrium with the mouth wall saturation. These findings are in good agreement with the experimental results reported by Ferrus et al. (11). The calculated results of the intra-

airway relative humidity (Fig. 11) showed that the air became 99.5% saturated at the 2nd generation during inspiration. At the end of expiration it remained almost at equilibrium with the wall (Fig. 12). The results showed that there was no supersaturation at inspiration or expiration. Supersaturation was proposed in the theoretical work by Ferron et al. (8) for nasal breathing, when the relative humidity of the inspired air was >50% or the inspired temperature was <20°C.

The important findings in the present work are: *1*) the airstream equilibrates with the airway wall before it reaches body conditions (37°C, 43.42 mg/l); *2*) the conditioning of the air for mouth breathing of room to warm conditions involves not only the upper airways but a number of generations of the bronchial tree, depending mainly on the ventilation; *3*) the airway wall conditions depend on the inspired conditions and the ventilation; and *4*) the airway wall, at least for the upper airways, is likely to be unsaturated.

APPENDIX A

Analytical Solution of the Equation of the Model

The equation of the model describing the transfer of heat and water vapor between the moving air and the surface of a circular tube as a function of radius and time is

$$\frac{\partial X}{\partial t} = D\left(\frac{1}{r}\frac{\partial X}{\partial r} + \frac{\partial^2 X}{\partial r^2}\right) \qquad (A1)$$

This was solved for $X(r,\bar{t})$, which represents either heat or water vapor concentration, as a function of r and $\bar{t}$.

The boundary conditions are

$$X(r,0) = f(r) \qquad 0 < r < R_w \qquad (A2)$$

$$X(R_w,\bar{t}) = X_w \qquad \bar{t} > 0 \qquad (A3)$$

Let $X = R(r)\,T(\bar{t})$. Then

$$R\,T'(\bar{t}) = D\left[\frac{1}{r}R'(r)\,T + R''(r)\,T(\bar{t})\right] \qquad (A4)$$

Dividing by $D\,R\,T$ gives

$$\frac{T'}{T\,D} = \frac{R''}{R} + \frac{1}{r}\frac{R'}{R} \qquad (A5)$$

Setting each side equal to $-\lambda^2$ gives

$$T' + D\lambda^2 T = 0 \qquad (A6)$$

and

$$R'' + \frac{1}{r}R' + \lambda^2 R = 0 \qquad (A7)$$

Solution of *Eq. A6* gives

$$T = C_1\, e^{-D\lambda^2\bar{t}} \qquad (A8)$$

where C_1 is a constant.

To solve $R'' + 1/r\,R' + \lambda^2 R = 0$, let $\lambda r = u$. Hence

$$\frac{d^2R}{du^2} + \frac{1}{u}\frac{dR}{du} + R = 0 \qquad (A9)$$

Equation A9 is Bessel's differential equation of order 0. The general solution is

$$R = C_2 J_0(u) + C_3 Y_0(u) \qquad (A10)$$

where C_2 and C_3 are constants and Y_0 is the Bessel function of the second kind of order 0.

Substituting u in *Eq. A10* gives

$$R = C_2 J_0(\lambda r) + C_3 Y_0(\lambda r) \qquad (A11)$$

When $r = 0$, $Y_0(\lambda r)$ is infinite and $C_3 = 0$. Hence

$$X(r,\bar{t}) = A e^{-D\lambda^2\bar{t}}\, J_0(\lambda r) \qquad (A12)$$

where A is a constant. The function $J_0(\lambda r)$ is similar to a trigonometric function $\cos(\lambda r)$ and has an infinite number of roots $\lambda_n r$, namely, $\lambda_1 r = 2.4048$, $\lambda_2 r = 5.5201$, $\lambda_3 r = 8.6537$, etc., for which $J_0(\lambda_n r) = 0$.

Therefore a particular solution is of the form

$$X(r,\bar{t}) = A_n e^{-D\lambda_n^2\bar{t}}\, J_0(\lambda_n r) \qquad (A13)$$

Because there is an infinite number of particular solutions, the general solution consists of a series of solutions

$$X(r,\bar{t}) = \sum_{n=1}^{\infty} A_n e^{-D\lambda_n^2\bar{t}} J_0(\lambda_n r) \qquad (A14)$$

From *Eq. A2*, $f(r) = \sum_{n=1} A_n J_0(\lambda_n r)$. The values of A_n are determined by multiplying both sides by $rJ_0(\lambda_m r)$ and integrating from 0 to R_w. Therefore

$$\int_0^{R_w} f(r) r J_0(\lambda_m r)\,dr = \sum_{n=1}^{\infty} A_n \int_0^{R_w} r J_0(\lambda_m r) J_0(\lambda_n r)\,dr$$

When $n = m$, then

$$\int_0^{R_w} r J_0(\lambda_n r) J_0(\lambda_n r)\,dr = \frac{1}{2} R_w^2 [J_1(\lambda_n R_w)]^2$$

Hence

$$A_n = \frac{2\int_0^{R_w} r f(r) J_0(\lambda_n r)\,dr}{R_w^2 [J_1(\lambda_n R_w)]^2}$$

When $f(r) = X_o$ (constant)

$$A_n = \frac{2X_o J_1(\lambda_n R_w)}{R_w \lambda_n [J_1(\lambda_n R_w)]^2} = \frac{2X_o}{R_w \lambda_n J_1(\lambda_n R_w)} \qquad (A15)$$

To help in evaluating the values of A_n, a new function $P(r,t)$ is introduced. Let $P(r,\bar{t}) = X_w - X(r,\bar{t})$. Therefore solution of *Eq. A1* with $P(r,\bar{t})$ is

$$P(r,\bar{t}) = \sum_{n=1}^{\infty} A_n e^{-D\lambda_n^2\bar{t}} J_0(\lambda_n r) \qquad (A16)$$

When $\bar{t} = 0$, $P(r,\bar{t}) = X_w - X(r,0)$. However, from the initial condition it follows that $X(r,0) = X_o$ and $P(r,0) = X_w - X_o$. Hence

$$A_n = \frac{2(X_w - X_o)}{R_w \lambda_n J_1(\lambda_n R_w)} \qquad (A17)$$

At the wall, $P(R_w,0) = X_w - X(R_w,0)$. But $X(R_w,0) = X_w$. Therefore, $P(R_w,0) = 0$ and $J_0(\lambda_n R_w) = 0$, where the values of λ_n are the zero positive roots. Hence

$$X_w - X(r,\bar{t}) = \sum_{n-1}^{\infty} \frac{2(X_w - X_o) J_0(\lambda_n r)}{\lambda_n R_w J_1(\lambda_n R_w)}\, e^{-D\lambda_n^2\bar{t}}$$

and

$$X(r,\bar{t}) = X_w - 2(X_w - X_o) \sum_{n=1}^{\infty} \frac{J_0(\lambda_n r)\, e^{-D\lambda_n^2 \bar{t}}}{\lambda_n R_w J_1(\lambda_n R_w)} \quad (A18)$$

Calculation of Mean $X(r,\bar{t})$

The mean temperature and water vapor concentration of a cross section is calculated as follows (16)

$$\begin{aligned}
&\text{mean } X(r,\bar{t}) \\
&= \frac{2\pi}{\pi R_w^2} \int_0^{R_w} rX(r,\bar{t})dr \\
&= \frac{2}{R_w^2} \int_0^{R_w} r\left[X_w - 2(X_w - X_o) \sum_{n=1}^{\infty} \frac{J_0(\lambda_n r)\, e^{-D\lambda_n^2 \bar{t}}}{\lambda_n R_w J_1(\lambda_n R_w)}\right] dr \\
&= \frac{2}{R_w^2} \int_0^{R_w} rX_w dr - \frac{2}{R_w^2} \int_0^{R_w} 2(X_w - X_o) \\
&\quad \cdot \sum_{n=1}^{\infty} \frac{rJ_0(\lambda_n r)\, e^{-D\lambda_n^2 \bar{t}}}{\lambda_n R_w J_1(\lambda_n R_w)} dr \\
&= X_w \frac{4(X_w - X_o)}{R_w^2} \int_0^{R_w} \sum_{n=1}^{\infty} \frac{rJ_0(\lambda_n r) e^{-D\lambda_n^2 \bar{t}}}{\lambda_n R_w J_1(\lambda_n R_w)} dr \\
&= X_w - \frac{4(X_w - X_o)}{R_w^2} \sum_{n-1}^{\infty} \int_0^{R_w} \frac{rJ_0(\lambda_n r)\, e^{-D\lambda_n^2 \bar{t}}}{\lambda_n R_w J_1(\lambda_n R_w)} dr
\end{aligned} \quad (A19)$$

Let $\lambda_n r = K$. Then $r = K/\lambda_n$ and $dr = dK/\lambda_n$. Substituting for r and dr gives

$$\begin{aligned}
&\text{mean } X(r,\bar{t}) \\
&= X_w - \frac{4(X_w - X_o)}{R_w^2} \sum_{n=1}^{\infty} \int_0^{\lambda_n R_w} \frac{KJ_0(K) e^{-D\lambda_n^2 \bar{t}}}{\lambda_n^3 R_w J_1(\lambda_n R_w)} dK \\
&= X_w - \frac{4(X_w - X_o)}{R_w^2} \sum_{n=1}^{\infty} \left[\frac{KJ_1(K)\, e^{-D\lambda_n^2 \bar{t}}}{\lambda_n^3 R_w J_1(\lambda_n R_w)}\right]^{\lambda_n R_w} \\
&= X_w - \frac{4(X_w - X_o)}{R_w^2} \sum_{n=1}^{\infty} \frac{\lambda_n R_w J_1(\lambda_n R_w) e^{-D\lambda_n^2 \bar{t}}}{\lambda_n^3 R_w J_1(\lambda_n R_w)} \\
&= X_w - \frac{4(X_w - X_o)}{R_w^2} \sum_{n=1}^{\infty} \frac{e^{-D\lambda_n^2 \bar{t}}}{\lambda_n^2}
\end{aligned} \quad (A20)$$

Therefore, the mean cross-sectional temperature and water vapor concentration can be calculated according to *Eq. A20.*

APPENDIX B

Airway Wall Temperature

It was considered that the wall temperatures would approach the core temperature in an asymptotic manner and that they would be a function of T_I and the ratio of the distance and airflow rate in an airway (8)

$$T_w = T_m + (37 - T_m)(1 - e^{-AL/\dot{V}}) \quad (B1)$$

T_m has not been measured, but it can be assumed to be close to T_E at the end of expiration. McCutchan and Taylor (18) derived an empirical equation for T_E when T_I varies from room to high temperature

$$T_E = 32.6 + 0.066T_I + 0.20\ W_I \quad (B2)$$

where W_I is measured in kilograms per kilogram dry air. This T_E is independent of ventilation. Ferrus et al. (11) proposed *Eq. B3* to predict the expired temperature

$$T_E = 26 + 0.25T_I \quad (B3)$$

for inspired conditions T_I = 10–40°C and 50% relative humidity. More recent experimental data, however, using a dividing valve to eliminate the heating or cooling of the valve and the measuring equipment by the previous respiratory half cycle, shows that T_E is a function of ventilation (20). These data are supported by the finding of Ferrus et al. (10) that the expired water vapor concentration depends also on ventilation. We have modified the equation of Ferrus et al. (11) as

$$T_m = B + 0.25T_I - C\dot{V}E \quad (B4)$$

The constants B and C were found by simultaneous fitting to obtain T_m between 32.9 and 30.4°C for $\dot{V}E$ 15 and 100 l/min. These limits for T_m were chosen because they were the air temperatures observed experimentally at the glottis during expiration (20). We found the best fit as

$$T_m = 25.5 + 0.25T_I - 0.018\dot{V}E \quad (B5)$$

To achieve self-consistency, A in *Eq. B1* was iterated until the smallest variation in T_m was found for a fixed $\dot{V}E$ and experimental T_w (20) at different locations.

This expression was substituted into *Eq. B1* and values of A were sought by simultaneous fitting of T_w at 15 and 100 l/min to obtain the minimum difference between experimental (20) and theoretical values. It was found that it was necessary to make A a function of ventilation too.

$$A = 0.00564\dot{V}E + 0.276 \quad \text{during inspiration}$$

$$A = 0.00564\dot{V}E + 0.336 \quad \text{during expiration}$$

It should be emphasized that the method to calculate T_w is entirely empirically based. Nevertheless, it is reasonable to assume both on physical and physiological grounds that T_w is a function of T_I, $\dot{V}E$, and depth in the respiratory tract and that they should be somewhat different during expiration and inspiration.

APPENDIX C

Additional Diffusivity

In a disturbed laminar flow, in addition to the heat and water transport by conduction and diffusion there is also a convective element, the magnitude of which depends on the level of turbulence at a particular location. It is reasonable to model the enhancement of the transport processes by the use of additional diffusivity D_a (8), which would depend on the location and the airflow rate. Initially, values of D_a at pharynx and larynx of 2, 3, 4, and 5 for $\dot{V}E$ 15, 30, 60, and 100 l/min were used, and these were increased to 4, 6, 8, and 10 at glottis and past it. These D_a values gave reasonable agreement with the experimental data of McFadden et al. (20) when values of T_w were used as explained in APPENDIX B. It was found that the plot of ln D_a vs. airflow rate $\dot{V}$ was linear

$$\ln D_a = \ln a + n \ln \dot{V}$$

The values of the constants a and n were found by fitting D_a values for ventilations of 30 and 60 l/min

$$n = 0.41$$

$$a = 0.177 \quad \text{for pharynx and larynx}$$

$$a = 0.354 \quad \text{for glottis and rest of airways}$$

The authors thank Dr. Klaus Schindhelm of the University of New South Wales for support throughout this work.

Address for reprint requests: I. Gonda, Dept. of Pharmacy, Sydney Univ., Sydney, NSW 2006, Australia.

Received 6 September 1988; accepted in final form 27 February 1990.

REFERENCES

1. ANDERSON, S. D., R. E. SCHOEFFEL, J. L. BLACK, AND E. DAVISKAS. Airway cooling as the stimulus to exercise-induced asthma: a re-evaluation. *Eur. J. Respir. Dis.* 67: 20–30, 1985.
2. ANDERSON, S. D., R. E. SCHOEFFEL, R. FOLLET, C. P. PERRY, E. DAVISKAS, AND M. KENDALL. Sensitivity to heat and water loss at rest and during exercise in asthmatic patients. *Eur. J. Respir. Dis.* 63: 459–471, 1982.
3. BRANCATISANO, T., P. W. COLLETT, AND L. A. ENGEL. Respiratory movements of the vocal chords. *J. Appl. Physiol.* 54: 1269–1276, 1983.
4. CHEN, W. Y., AND D. J. HORTON. Heat and water loss from the airways and exercise-induced asthma. *Respiration* 34: 305–313, 1977.
5. COLE, G. W., AND N. R. SCOTT. A mathematical model of the dynamic heat transfer from the respiratory tract of a chicken. *Bull. Math. Biol.* 39: 415–433, 1977.
6. COLLINS, J. C., T. C. PILKINGTON, AND K. SCHMIDT-NIELSEN. A model of respiratory heat transfer in a small mammal. *Biophys. J.* 11: 886–913, 1971.
7. DIEM, K. *Scientific Tables* (6th ed.). Ardsley, NY: Geigy Pharmaceuticals, 1968.
8. FERRON, G. A., B. HAIDER, AND W. G. KREYLING. A method for the approximation of the relative humidity in the upper airways. *Bull. Math. Biol.* 47: 565–589, 1985.
9. FERRON, G. A., B. HAIDER, AND W. G. KREYLING. Inhalation of salt aerosol particles. I. Estimation of the temperature and relative humidity of the air in the human upper airways. *J. Aerosol Sci.* 19: 343–363, 1988.
10. FERRUS, L., D. COMMENGES, J. GIRE, AND P. VARENE. Respiratory water loss as a function of ventilatory or environmental factors. *Respir. Physiol.* 56: 11–20, 1984.
11. FERRUS, L., H. GUENARD, G. VARDON, AND P. VARENE. Respiratory water loss. *Respir. Physiol.* 39: 367–381, 1980.
12. HANNA, L. M., AND P. SCHERER. A theoretical model of localised heat and water transport in the human respiratory tract. *J. Biomech. Eng.* 108: 19–27, 1986.
13. HANNA, L. M., AND P. SCHERER. Regional control of local airway heat and water vapor losses. *J. Appl. Physiol.* 61: 624–632, 1986.
14. INGENITO, E. P., J. SOLWAY, E. R. MCFADDEN, JR., B. M. I. PICHURKO, F. BOWMAN, D. MICHAELS, AND J. M. DRAZEN. Indirect assessment of mucosal surface temperatures in the airways: theory and tests. *J. Appl. Physiol.* 63: 2075–2083, 1987.
15. INGENITO, E. P., J. SOLWAY, E. R. MCFADDEN, JR., B. M. I. PICHURKO, E. G. CRAVALHO, AND J. M. DRAZEN. Finite difference analysis of respiratory heat transfer. *J. Appl. Physiol.* 61: 2252–2259, 1986.
16. JACOB, M. *Heat Transfer.* New York: Wiley, 1962, vol. 1.
17. JAEGER, M. J., AND H. MATTHYS. The pressure flow characteristics of the human airways. In: *Airway Dynamics*, edited by A. Bohuys. Springfield, IL: Thomas, 1970.
18. MCCUTCHAN, J. W., AND C. L. TAYLOR. Respiratory heat exchange with varying temperature and humidity of inspired air. *J. Appl. Physiol.* 4: 121–135, 1951.
19. MCFADDEN, E. R., JR., D. M. DENISON, J. F. WALLER, B. I. ASSOUFI, A. PEACOCK, AND T. SOPWITH. Direct recordings of the temperatures in the tracheobronchial tree in normal man. *J. Clin. Invest.* 69: 700–705, 1982.
20. MCFADDEN, E. R., JR., B. M. PICHURKO, H. F. BOWMAN, E. INGENITO, S. BURNS, N. DOWLING, AND J. SOLWAY. Thermal mapping of the airways in humans. *J. Appl. Physiol.* 58: 564–570, 1985.
21. PEDLEY, T. J., M. F. SUDLOW, AND R. C. SCHROTER. Gas flow and mixing in the airways. In: *Bioengineering Aspects of the Lung*, edited by J. B. West. New York: Dekker, 1977, chapt. 3, p. 163–265. (Lung Biol. Health Dis. Ser.)
22. SAIDEL, G. M., K. L. KRUSE, AND F. P. PRIMIANO, JR. Model simulation of heat and water transport dynamics in an airway. *J. Biomech. Eng.* 105: 188–193, 1983.
23. SCHROTER, R. C., AND M. F. SUDLOW. Flow patterns in models of the human bronchial airways. *Respir. Physiol.* 7: 341–355, 1969.
24. SEYMOUR, R. S. Convective heat transfer in the respiratory systems of panting animals. *J. Theor. Biol.* 35: 119–127, 1972.
25. SOLWAY, J., B. M. PICHURKO, E. P. INGENITO, E. R. I. MCFADDEN, JR., H. FANTAC, R. H. INGRAM, JR., AND J. M. DRAZEN. Breathing pattern affects airway wall temperature during cold air hyperpnoea in humans. *Am. Rev. Respir. Dis.* 132: 853–857, 1985.
26. SWIFT, D. L., AND D. F. PROCTOR. Access of air to the respiratory tract. In: *Respiratory Defense Mechanisms*, edited by J. D. Brain, D. F. Proctor, and L. M. Reid. New York: Dekker, 1977, pt. I, chapt. 3, p. 63–94. (Lung Biol. Health Dis. Ser.)
27. TABKA, Z., A. B. JEBRIA, AND H. GUENARD. Effect of breathing dry warm air on respiratory water loss at rest and during exercise. *Respir. Physiol.* 67: 115–125, 1987.
28. TSU, M. E., A. L. BABB, D. D. RALPH, AND M. P. HLASTALA. Dynamics of heat, water, and soluble gas exchange in the human airways. I. A model study. *Ann. Biomed. Eng.* 16: 547–571, 1988.
29. ULTMAN, J. S. Gas mixing in the pulmonary airways. *Ann. Biomed. Eng.* 9: 513–527, 1981.
30. ULTMAN, J. S. Gas transport in the conducting airways. In: *Gas Mixing and Distribution in the Lung*, edited by L. A. Engel and M. Paiva. New York: Dekker, 1985, p. 63–136. (Lung Biol. Health Dis. Ser.)
31. WEIBEL, E. R. Morphometrics of the lung. In: *Handbook of Physiology. Respiration.* Washington, DC: Am. Physiol. Soc., 1964, sect. 3, chapt. 7, p. 285–307.